Published for SISSA by Springer

Received: *August 20, 2021*
Revised: *December 10, 2021*
Accepted: *December 21, 2021*
Published: *January 14, 2022*

JHEP01(2022)069

Search for the radiative $\Xi_b^- \to \Xi^-\gamma$ decay

The LHCb collaboration

E-mail: lgarciam@cern.ch

Abstract: The first search for the rare radiative decay $\Xi_b^- \to \Xi^-\gamma$ is performed using data collected by the LHCb experiment in proton-proton collisions at a center-of-mass energy of 13 TeV, corresponding to an integrated luminosity of $5.4\,\text{fb}^{-1}$. The $\Xi_b^- \to \Xi^- J/\psi$ channel is used as normalization. No $\Xi_b^- \to \Xi^-\gamma$ signal is found and an upper limit of $\mathcal{B}(\Xi_b^- \to \Xi^-\gamma) < 1.3 \times 10^{-4}$ at 95% confidence level is obtained.

Keywords: B physics, Flavor physics, Hadron-Hadron scattering (experiments), Rare decay

ArXiv ePrint: 2108.07678

https://doi.org/10.1007/JHEP01(2022)069

Contents

JHEP01(2022)069

1 Introduction

The $b \to s\gamma$ transition, depicted in figure 1, is a flavor-changing neutral-current process characterized by the emission of a photon in the final state. Decays involving this feature are also known as radiative decays. The effective Hamiltonian in the operator product expansion formalism describing $b \to s\gamma$ transitions at leading order is given by

$$\mathcal{H}_{\text{eff}} = -\frac{G_F}{\sqrt{2}} V_{ts}^* V_{tb} (\mathcal{C}_7 \mathcal{O}_7 + \mathcal{C}_7' \mathcal{O}_7') \,, \tag{1.1}$$

where $\mathcal{O}_7$ ($\mathcal{O}_7'$) represents the left (right) projection of the electromagnetic penguin operator, which corresponds to the emission of a left (right)-handed photon. The strength of each contribution is encoded in the Wilson coefficients $\mathcal{C}_7$ and $\mathcal{C}_7'$. In the SM, the W^- boson only couples to left-handed quarks and, thus, the only source of right-handed photons is due to helicity flips. The ratio of right- and left-handed amplitudes is expected to be $\mathcal{O}(m_s/m_b)$. Thus, the SM predicts a negligible contribution of the right-handed operator $\mathcal{O}_7'$. Measuring branching fractions, angular and charge-parity-violating observables in $b \to s\gamma$ transitions enables testing the presence of right-handed contributions. Several analyses focusing on B-meson decays have explored this field [1–5].

Radiative decays of b-baryons provide access to the photon polarization due to the spin ½ ground state, the absence of flavor mixing and the presence of two spectator quarks. Therefore, b-baryon decays provide complementary measurements to those performed with radiative B-meson decays [6].

The branching fraction of the $\Lambda_b^0 \to \Lambda\gamma$ decay mode has been recently measured for the first time [7] and constitutes the first radiative b-baryon decay observed.[1] Further radiative

[1] Charge-conjugated processes are implied throughout this paper.

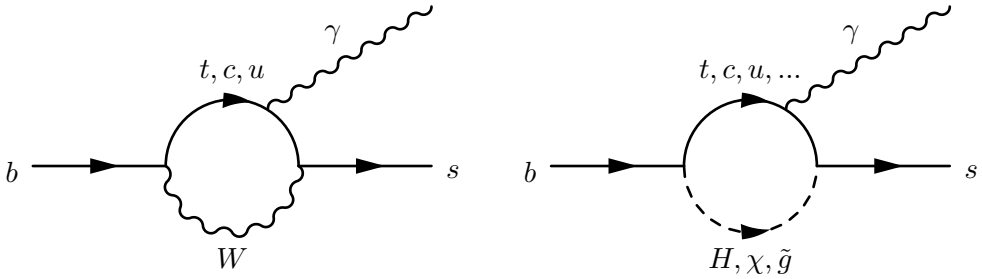

Figure 1. The $b \to s\gamma$ penguin diagram, mediated by SM particles (left) and BSM particles (right).

b-baryon decays can be studied with the LHCb detector, providing complementary tests of the photon polarization in the SM. This paper focuses on the search for the $\Xi_b^- \to \Xi^-\gamma$ decay mode, which is also mediated by the $b \to s\gamma$ transition. The LHCb experiment provides unique conditions for studying the $\Xi_b^- \to \Xi^-\gamma$ mode thanks to the large production of b-baryons at the LHC [8, 9] and the excellent performance of the detector optimized for the analysis of b-hadron decays. Additionally, previous measurements at LHCb involving radiative B meson [1–5] and b-baryon [7] decays motivates the search for new radiative baryonic modes, such as the $\Xi_b^- \to \Xi^-\gamma$ decay.

The rare radiative b-baryon decay $\Xi_b^- \to \Xi^-\gamma$ has not yet been observed. Using light-cone sum rules, its branching fraction, $\mathcal{B}(\Xi_b^- \to \Xi^-\gamma)$, is predicted to be $(3.03 \pm 0.10) \times 10^{-4}$ [10]. This prediction is larger than the branching fraction of other radiative decays ($\mathcal{B} \sim \mathcal{O}(10^{-5})$) [7, 11, 12]. A more recent study uses SU(3) flavor symmetry rules to predict $\mathcal{B}(\Xi_b^- \to \Xi^-\gamma) = (1.23 \pm 0.64) \times 10^{-5}$ [13]. This second prediction uses the measurement of $\mathcal{B}(\Lambda_b^0 \to \Lambda\gamma)$ and thus it has a smaller dependency on estimated form factors. A measurement of the branching fraction of this decay could discriminate different approaches used in the theoretical predictions. This could help to estimate form-factors at low q^2 (photon pole) for the semileptonic decay $\Xi_b^- \to \Xi^-\mu^+\mu^-$ [14]. Furthermore, the possible signal obtained could be used to perform a measurement of the photon polarization [15].

The data sample analyzed in this paper corresponds to an integrated luminosity of $5.4\,\text{fb}^{-1}$ of proton-proton (pp) collisions at a center-of-mass energy of 13 TeV, collected by the LHCb detector. Potential experimenters' bias is avoided by validating the analysis procedure before inspecting the results. A normalization channel sharing the same hadronic part of the final state as the radiative decay is used to cancel potential systematic effects arising from detector efficiencies and the limited knowledge on the Ξ_b^- production, $f_{\Xi_b^-}$. The normalization channel is chosen to be the $\Xi_b^- \to \Xi^- J/\psi$ decay.

2 LHCb detector

The LHCb detector [16, 17] is a single-arm forward spectrometer covering the pseudorapidity range $2 < \eta < 5$, designed for the study of particles containing b or c quarks. The detector includes a high-precision tracking system consisting of a silicon-strip vertex detector surrounding the pp interaction region, a large-area silicon-strip detector located

JHEP01(2022)069

upstream of a dipole magnet with a bending power of about 4 Tm, and three stations of silicon-strip detectors and straw drift tubes placed downstream of the magnet. The tracking system provides measurements of the momentum of charged particles with a relative uncertainty that varies from 0.5% at low momentum to 1.0% at 200 GeV/c. The minimum distance of a track to a primary pp collision vertex (PV), the impact parameter, is measured with a resolution of $(15 \pm 29/p_{\mathrm{T}})\,\mu$m, where p_{T} is the component of the momentum transverse to the beam, in GeV/c. The PV is reconstructed by forming a common vertex from a large number of tracks, consistent with originating from a pp collision [18]. Different types of charged hadrons are distinguished using information from two ring-imaging Cherenkov detectors. Photons, electrons and hadrons are identified by a calorimeter system consisting of scintillating-pad and preshower detectors, an electromagnetic and a hadronic calorimeter. Charged and neutral clusters in the electromagnetic calorimeter are discerned by extrapolating the tracks reconstructed by the tracking system to the calorimeter plane. Photons and neutral pions are distinguished by cluster shape, energy and mass distributions. Muons are identified by a system composed of alternating layers of iron and multiwire proportional chambers. Due to the photon energy resolution, b-hadron decays with a high-energy photon in their final state are reconstructed with a b-hadron mass resolution around 100 MeV/c^2 [3].

The online event selection is performed by a trigger system [19], consisting of a hardware stage, which uses information from the calorimeter and muon systems, followed by two software stages, which apply a partial and a full event reconstruction. At the hardware trigger stage, events are required to have a high-p_{T} photon or electron, detected in the electromagnetic calorimeter as a cluster of transverse energy (E_{T}) with a threshold that varied between 2.1 and 3.0 GeV during the data-taking period. The first stage of the software trigger requires a track well separated from any PV, and with a p_{T} higher than 1 GeV/c. At the second stage of the software trigger, the full decay chain is reconstructed to identify decays consistent with the signal mode. Only events signal candidate fulfilling the trigger requirements are kept.

Simulation is used to develop the selection strategy, compute the efficiency and determine the shape of the invariant-mass distribution of the signal decays. In the simulation, pp collisions are generated using Pythia [20, 21] with a specific LHCb configuration [22]. Decays of unstable particles are described by EvtGen [23], in which final-state radiation is generated using Photos [24]. The interaction of the generated particles with the detector, and its response are simulated using the Geant4 toolkit [25, 26], as described in ref. [27]. To save computing resources, the simulated signal decay is superimposed to a limited set of simulated underlying interactions which are used multiple times [28].

3 Selection

The reconstruction of the $\Xi_b^- \to \Xi^-\gamma$ decay, with $\Xi^- \to \Lambda\pi^-$ and $\Lambda \to p\pi^-$, involves the combination of two tracks with opposite charges originating from a common displaced vertex, and compatible with the p and π^- hypotheses. This is identified as a Λ baryon, which is combined with a π^- track to form the Ξ^- candidate. The Ξ_b^- candidate is in

JHEP01(2022)069

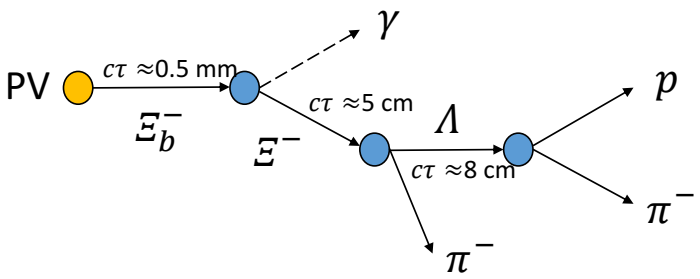

Figure 2. Topology of the $\Xi_b^- \to \Xi^-\gamma$ decay, including three displaced vertices, with $c\tau$ of each particle given.

turn reconstructed as the combination of an energetic photon and the reconstructed Ξ^- candidate. A sketch of the full decay chain, which includes three independent displaced vertices, is shown in figure 2.

High-quality tracks inconsistent with originating from the PV are used for the reconstruction. For events with multiple PVs, the PV with the lowest impact parameter with respect to the candidate is used. Because of the long lifetime and large Lorentz boost, most of the Λ and Ξ^- baryons decay outside the vertex detector. However, due to trigger limitations, only decays that occur inside the vertex detector can be considered. Particle identification requirements, based on a multivariate analysis technique, are applied to the charged particles [29]. Proton and pion candidates with a minimum transverse momentum of 630 MeV/c and 250 MeV/c, respectively, are used to form a Λ candidate. The proton-pion system is required to have a mass within 6 MeV/c^2 of the known Λ mass [30] and a p_{T} larger than 1.5 GeV/c. The Λ candidate is then combined with a pion candidate with $p_{\mathrm{T}} > 130$ MeV/c to form a Ξ^- candidate. This candidate is required to have decayed within 400 mm of the PV, to have a p_{T} larger than 2 GeV/c and a mass, $m(\pi^-\pi^-p)$ in the range 1310–1332 MeV/c^2 around the known value of the Ξ^- mass of 1321.71 ± 0.07 MeV/c^2 [30]. After the trigger and offline requirements, a clean sample of Ξ^- candidates is obtained. The distribution of the mass of Ξ^- candidates is shown in figure 3. Photon candidates are reconstructed from energy deposits in the electromagnetic calorimeter not associated to any track. Background due to photons from π^0 decays is rejected by a dedicated algorithm [31]. The Ξ^- candidate is combined with a photon candidate with E_{T} larger than 4 GeV. Due to the unknown photon direction and the long lifetime of the Ξ^- baryon, the Ξ_b^- decay vertex cannot be determined. Consequently, the Ξ_b^- trajectory is calculated assuming the photon originates from the PV with the smallest distance of closest approach with respect to the Ξ^- trajectory. This is a good approximation given the short decay time of the Ξ_b^- baryon. The γ and Ξ^- momenta are then combined to reconstruct the Ξ_b^- candidate. The Ξ_b^- candidate must have p_{T} larger than 4 GeV/c and a mass within 800 MeV/c^2 of its known mass [30]. The distance of closest approach between the Ξ_b^- and the Ξ^- trajectories must be < 50 μm.

The combinatorial background, formed by random combinations of final-state particles, is suppressed by using a boosted decision tree (BDT) [32], employing the XGBOOST algorithm [33]. The BDT classifier is trained using simulated samples of $\Xi_b^- \to \Xi^-\gamma$ decays as signal, and candidates from data samples with the $\Xi^-\gamma$ mass above 6.1 GeV/c^2

JHEP01(2022)069

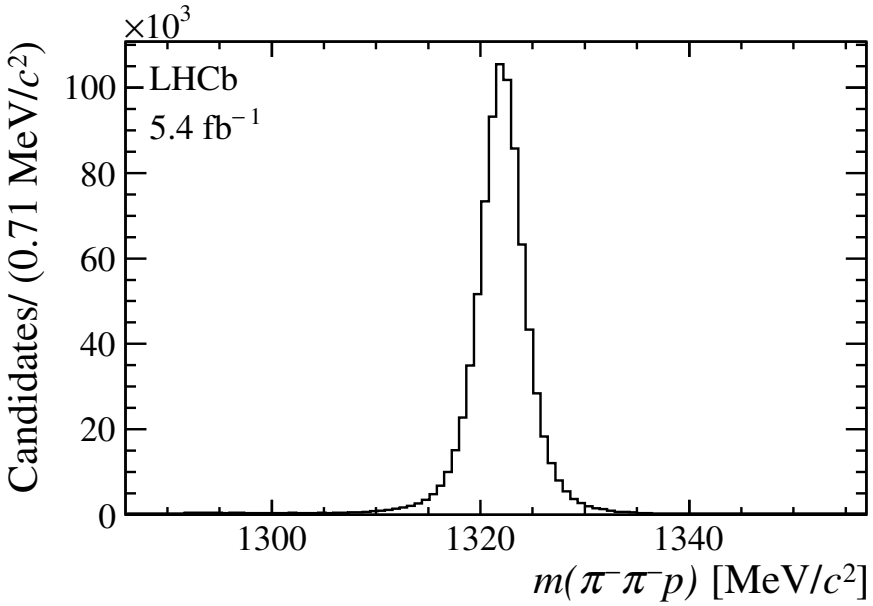

Figure 3. Mass distribution $m(\pi^-\pi^-p)$ showing the $\Xi^- \to \Lambda\pi^-$ signal for events satisfying the trigger and the offline requirements described in the text for $\Xi_b^- \to \Xi^-\gamma$ decays.

as a background proxy. The k-folding cross-validation technique [34] with $k = 5$ is used to avoid overfitting the BDT model. The variables used to train the BDT classifier are: the transverse momentum and the separation from the PV of the signal decay products; the photon pseudorapidity; the distance of closest approach between the Ξ^- decay products and between the Ξ_b^- and Ξ^- flight directions; and the $p_{\rm T}$ asymmetry of the Ξ^- and the γ candidates. The $p_{\rm T}$ asymmetry for a given particle is computed as the normalized difference between the summed momenta of all tracks within a cone of 1 rad around the particle direction, and the momentum of the particle. The above variable discriminates against partially reconstructed backgrounds, consisting of decays with additional particles in the final state that have not been reconstructed. As the BDT classifier is trained using simulation, good agreement between the simulation and data is needed. This is validated using the $\Lambda_b^0 \to J/\psi p K^-$ and $B^0 \to K^*\gamma$ control modes employing the selection criteria described in refs. [35] and [3], respectively. The normalization channel $\Xi_b^- \to \Xi^- J/\psi$, with the selection described below, is also used for the same purpose. The event multiplicity, defined as the number of tracks per event, along with the b-baryon momentum and transverse momentum are corrected for discrepancies between simulation and data. These corrections are extracted from $\Lambda_b^0 \to J/\psi p K^-$ background-subtracted data and simulated samples. The BDT classifier is optimized by maximizing the Punzi figure of merit [36], $\epsilon_{\rm s}/(\sqrt{B} + 2.5)$, where $\epsilon_{\rm s}$ is the efficiency of the requirement on the BDT output extracted from simulated signal events, and B is the background yield from the high-mass sideband, extrapolated to the signal region. The chosen working point keeps 69% of the signal candidates, while suppressing about 98% of the combinatorial background.

JHEP01(2022)069

The online reconstruction of candidates from the $\Xi_b^- \to \Xi^- J/\psi$ normalization channel, with $J/\psi \to \mu^+\mu^-$, follows a different strategy as compared to the $\Xi_b^- \to \Xi^-\gamma$ signal channel. The muons, originating from inside the vertex detector, must pass the trigger for the normalization channel. This allows Λ and Ξ^- baryons decaying both inside and outside the vertex detector to be used. For the trigger selection of the normalization channel, events are required to either have a muon with a p_{T} above 1.5 GeV/c, or two muons with a transverse momentum product greater than 1.6 GeV$^2/c^2$. In the first software stage of the trigger, the event must have either a system of two well-identified oppositely charged muons with a large mass, $m(\mu^+\mu^-) > 2.7\,\mathrm{GeV}/c^2$, or at least one muon with $p_{\mathrm{T}} > 1$ GeV that is inconsistent with originating from any PV. In the second stage, events containing a $\mu^+\mu^-$-pair with a mass consistent with the known J/ψ mass [30], and with a vertex significantly displaced from any PV, are selected. The offline reconstruction follows similar criteria to the $\Xi_b^- \to \Xi^-\gamma$ selection. The J/ψ candidate is reconstructed from two oppositely-charged tracks compatible with the muon hypothesis. The mass of the $\mu^+\mu^-$ pair is required to be within a window of 60 MeV/c^2 around the known J/ψ mass [30]. In this case, the Ξ_b^- vertex is reconstructed with an improved b-baryon mass resolution, with respect to the radiative decay, due to a precise measurement of the muon momenta. The Ξ_b^- candidate is required to have a measured decay time between 0.3 and 1.4 ps, a mass within 300 MeV/c^2 of the Ξ_b^- measured mass [30] and a good quality decay vertex. Given the high purity of the $\Xi_b^- \to \Xi^- J/\psi$ sample after the described selection, no BDT selection is used.

4 Yield determination

The signal is isolated from the background components by a fit to the reconstructed Ξ_b^- mass distribution of the selected candidates. An unbinned maximum likelihood fit to the radiative, $\Xi_b^- \to \Xi^-\gamma$, and the normalization, $\Xi_b^- \to \Xi^- J/\psi$, decay modes are used. The signal-mass shape is modeled with a double-sided Crystal Ball probability density function [37], comprising a Gaussian core and a power-law tail at both sides. The parameters for the tails are extracted from a fit to simulated samples. In the mass fit to data, the peak position for the radiative and normalization channels is the same, while the peak width is related using a scaling factor defined as the ratio of the signal and normalization widths in simulation. Sources of non-combinatorial background are investigated using simulated samples. The narrow width of the Λ and Ξ^- baryons [30] and the clean sample of the latter (see figure 3) reduces the contamination from decays where one or more final state particles are misidentified, such as $\Omega_b^- \to \Omega^-\gamma$. No candidates from the partially reconstructed background $\Xi_b^- \to \Xi\eta$ with $\eta \to \gamma\gamma$ are expected in the selected data sample. There are no predictions for Ξ_b^- baryons decaying into π^0 mesons. This class of contamination is known to be suppressed in B^0 decays to $K^*\gamma$ and $K^*\pi^0$ final states, and the same is assumed in the baryon sector [30]. The only relevant background component is the combinatorial one, which is modeled with an exponential function. The mass fit is validated using pseudoexperiments with $\mathcal{B}(\Xi_b^- \to \Xi^-\gamma)$ hypotheses ranging from 10^{-5} to 10^{-3}.

JHEP01(2022)069

Parameter	Value
τ_{Ξ_b}	1.57 ± 0.04 ps [30]
$\tau_{\Lambda_b^0}$	1.47 ± 0.01 ps [30]
$\mathcal{B}(\Lambda_b^0 \to \Lambda J/\psi)$	$(3.36 \pm 1.11) \times 10^{-4}$ [39, 40]

Table 1. Input parameters used to compute the branching fraction $\mathcal{B}(\Xi_b^- \to \Xi^- J/\psi)$.

The branching fraction is determined as

$$\begin{aligned}\mathcal{B}(\Xi_b^- \to \Xi^-\gamma) &= \mathcal{B}(\Xi_b^- \to \Xi^- J/\psi)\mathcal{B}(J/\psi \to \mu^+\mu^-) \\ &\quad \times \frac{\epsilon(\Xi_b^- \to \Xi^- J/\psi)}{\epsilon(\Xi_b^- \to \Xi^-\gamma)} \frac{N(\Xi_b^- \to \Xi^-\gamma)}{N(\Xi_b^- \to \Xi^- J/\psi)} \\ &= \alpha N(\Xi_b^- \to \Xi^-\gamma)\,,\end{aligned} \tag{4.1}$$

where $\mathcal{B}$ indicates a branching fraction, N is the signal yield extracted from the mass fit, ϵ denotes the combined reconstruction and selection efficiency for the given decay and α is the single-event sensitivity. Calibration samples of $\Lambda \to p\pi^-$, $D^0 \to K^-\pi^+$, $J/\psi \to \mu^+\mu^-$ and $B^0 \to K^*\gamma$ are used to calculate the efficiencies of the particle identification requirements [29, 31]. The remaining selection and reconstruction efficiencies are determined from simulated samples.

The value of the $\Xi_b^- \to \Xi^- J/\psi$ branching fraction multiplied by the hadronization fraction of Ξ_b^- baryons, $f_{\Xi_b^-}$, is provided in ref. [30]. Due to the lack of precision in the $f_{\Xi_b^-}$ absolute value, the $\Xi_b^- \to \Xi^- J/\psi$ branching fraction is computed using the SU(3) relation $\Gamma(\Xi_b^- \to \Xi^- J/\psi) = (3/2 \pm 0.45) \times \Gamma(\Lambda_b^0 \to \Lambda J/\psi)$ [38] instead. The quoted uncertainty is typical for flavor SU(3) predictions. Combining the values listed in table 1, the computed value of $\mathcal{B}(\Xi_b^- \to \Xi^- J/\psi)$ is

$$\mathcal{B}(\Xi_b^- \to \Xi^- J/\psi) = \left(\frac{3}{2} \pm 0.45\right) \frac{\tau_{\Xi_b}}{\tau_{\Lambda_b^0}} \mathcal{B}(\Lambda_b^0 \to \Lambda J/\psi) = (5.4 \pm 2.4) \times 10^{-4}\,. \tag{4.2}$$

5 Results

Figure 4 shows the distribution of (top) the mass $m(\pi^-\pi^- p\gamma)$ for selected $\Xi^-\gamma$ and (bottom) $m(\pi^-\pi^- p\,\mu^+\mu^-)$ for selected $\Xi^- J/\psi$ candidates. The simultaneous mass fit to these mass distributions returns yields of $N(\Xi_b^- \to \Xi^-\gamma) = -3.6 \pm 3.9$ and $N(\Xi_b^- \to \Xi^- J/\psi) = 1407 \pm 52$. Using the yield for the normalization channel together with the other quantities of eq. (4.1), a single-event sensitivity of $\alpha = (7.9 \pm 3.6) \times 10^{-6}$ is obtained.

Systematic uncertainties on the measurement of the $\mathcal{B}(\Xi_b^- \to \Xi^-\gamma)$ value arise from several sources. The systematic effect due to the choice of the mass fit model is assessed by means of pseudoexperiments wherein the mass distribution is generated with an alternative model and fitted using the default model. The validation of fixing the value of the scale parameter relating the radiative and normalization channel resolutions is assessed by

JHEP01(2022)069

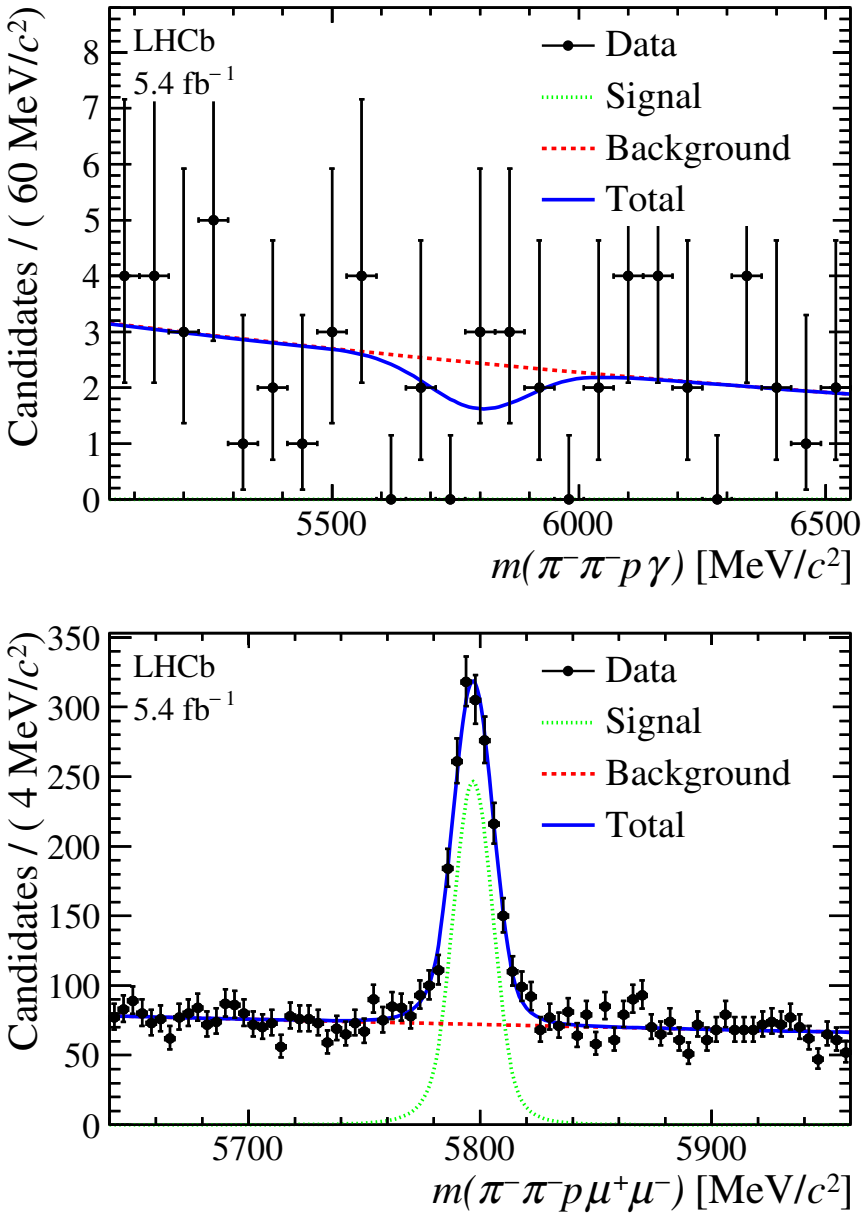

Figure 4. Distribution of (top) mass $m(\pi^-\pi^-p\gamma)$ for selected $\Xi^-\gamma$ ($\Xi^- \to \Lambda\pi^-$) and (bottom) $m(\pi^-\pi^-p\mu^+\mu^-)$ for selected $\Xi^- J/\psi$ ($J/\psi \to \mu^+\mu^-$) candidates. The projections of the simultaneous fit are overlaid.

JHEP01(2022)069

Source	Uncertainty (%)
Mass fit model (signal)	9.1
Mass fit model (background)	7.8
Efficiency ratio	4.6
Hardware trigger	10.0
Simulation/Data agreement	6.0
$\mathcal{B}(\Xi_b^- \to \Xi^- J/\psi)$	45.6
Sum in quadrature	48.7

Table 2. Dominant systematic uncertainties on the measurement of the branching fraction $\mathcal{B}(\Xi_b^- \to \Xi^-\gamma)$.

repeating the measurement considering possible differences between data and simulation. No deviation is found with respect to the nominal measurement and, thus, no systematic uncertainty is assigned to this effect. The uncertainty on the selection efficiencies, originating from the limited sample size, is propagated to the branching fraction and considered as a systematic uncertainty. The corrections applied to the simulation to improve the agreement with data are varied within their statistical uncertainty. The effect of a possible mismodeling of the radiative hardware level trigger is assessed by comparing the efficiency extracted from simulation and from a method using the $B^0 \to K^{*0}\gamma$ decay as a control channel. The limited precision of the external value of $\mathcal{B}(\Xi_b^- \to \Xi^- J/\psi)$ induces the largest systematic uncertainty. Table 2 summarizes the systematic uncertainties.

Since no $\Xi_b^- \to \Xi^-\gamma$ signal is observed, the Feldman-Cousins (FC) method [41] is used to set an upper limit on the value of $\mathcal{B}(\Xi_b^- \to \Xi^-\gamma)$. For the FC method, the relation between the true and fitted signal yield and the statistical uncertainty are determined from pseudoexperiments. The systematic uncertainty is added in quadrature to the statistical uncertainty. The value of $\mathcal{B}(\Xi_b^- \to \Xi^-\gamma)$ is calculated from the signal yield using eq. (4.1). From this set of values, the 95% confidence level (CL) is built and shown in figure 5.

Combining this study with the measured yield ratio, an upper limit is set

$$\mathcal{B}(\Xi_b^- \to \Xi^-\gamma) < 1.3\,(0.6) \times 10^{-4} \text{ at } 95\%\,(90\%) \text{ CL}\,.$$

This is the first limit on this decay channel. Because the systematic uncertainty from the normalization channel branching fraction is dominant, the ratio of the branching fractions is reported, where the total systematic reduces to 17%. Using the FC approach, an upper limit of

$$\frac{\mathcal{B}(\Xi_b^- \to \Xi^-\gamma)}{\mathcal{B}(\Xi_b^- \to \Xi^- J/\psi)} < 0.12\,(0.08) \text{ at } 95\%\,(90\%) \text{ CL}\,,$$

is set.

JHEP01(2022)069

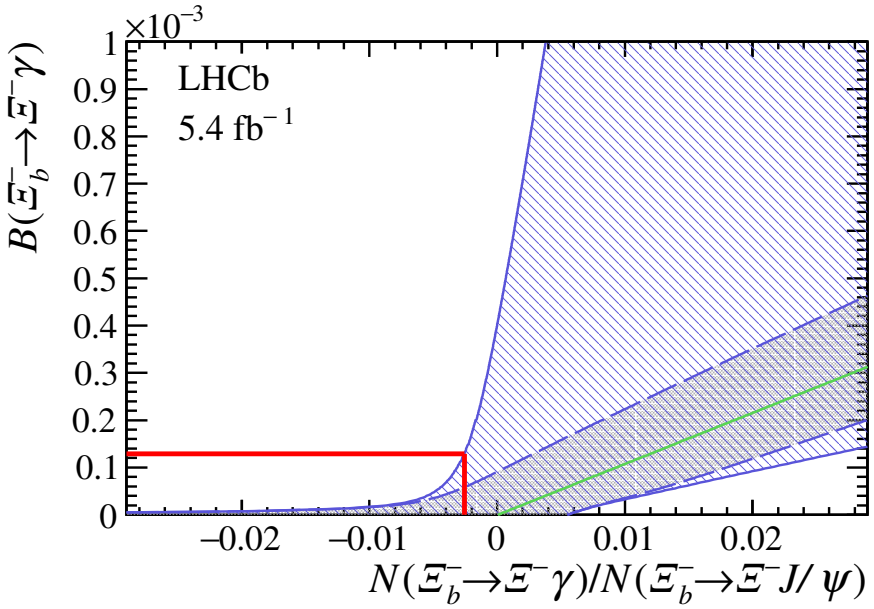

Figure 5. Confidence interval at 95% CL showing the upper limit for $\mathcal{B}(\Xi_b^- \to \Xi^-\gamma)$ as a function of the $\frac{N(\Xi_b^- \to \Xi^-\gamma)}{N(\Xi_b^- \to \Xi^- J/\psi)}$ ratio. The green line represents the relation between the yield and the branching fractions. The interval considering only the statistical uncertainty is shown by the dashed blue lines, while the full blue lines also includes the systematic uncertainties. The measured ratio of the yields and the upper limit on the branching fraction are represented by the red line.

6 Conclusion

The first search for b-baryon flavor-changing neutral-current radiative $\Xi_b^- \to \Xi^-\gamma$ decay is reported, using pp collision data at a center-of-mass energy of $\sqrt{s} = 13\,\text{TeV}$ collected by the LHCb experiment. The data set corresponds to an integrated luminosity of $5.4\,\text{fb}^{-1}$. No evidence for a signal is found. Upper limits at 90% and 95% CL of the value of $\mathcal{B}(\Xi_b^- \to \Xi^-\gamma)$ are reported, which are in slight tension with the predictions from light-cone sum rules [10] but are consistent with flavor-symmetry driven predictions from ref. [13].

Acknowledgments

We express our gratitude to our colleagues in the CERN accelerator departments for the excellent performance of the LHC. We thank the technical and administrative staff at the LHCb institutes. We acknowledge support from CERN and from the national agencies: CAPES, CNPq, FAPERJ and FINEP (Brazil); MOST and NSFC (China); CNRS/IN2P3 (France); BMBF, DFG and MPG (Germany); INFN (Italy); NWO (Netherlands); MNiSW and NCN (Poland); MEN/IFA (Romania); MSHE (Russia); MICINN (Spain); SNSF and SER (Switzerland); NASU (Ukraine); STFC (United Kingdom); DOE NP and NSF (U.S.A.). We acknowledge the computing resources that are provided by CERN, IN2P3 (France), KIT and DESY (Germany), INFN (Italy), SURF (Netherlands), PIC (Spain),

JHEP01(2022)069

GridPP (United Kingdom), RRCKI and Yandex LLC (Russia), CSCS (Switzerland), IFIN-HH (Romania), CBPF (Brazil), PL-GRID (Poland) and NERSC (U.S.A.). We are indebted to the communities behind the multiple open-source software packages on which we depend. Individual groups or members have received support from ARC and ARDC (Australia); AvH Foundation (Germany); EPLANET, Marie Skłodowska-Curie Actions and ERC (European Union); A*MIDEX, ANR, IPhU and Labex P2IO, and Région Auvergne-Rhône-Alpes (France); Key Research Program of Frontier Sciences of CAS, CAS PIFI, CAS CCEPP, Fundamental Research Funds for the Central Universities, and Sci. & Tech. Program of Guangzhou (China); RFBR, RSF and Yandex LLC (Russia); GVA, XuntaGal and GENCAT (Spain); the Leverhulme Trust, the Royal Society and UKRI (United Kingdom).

References

[1] LHCb collaboration, *Observation of photon polarization in the $b \to s\gamma$ transition*, *Phys. Rev. Lett.* **112** (2014) 161801 [arXiv:1402.6852] [INSPIRE].

[2] BELLE collaboration, *Search for $B_s^0 \to \gamma\gamma$ and a measurement of the branching fraction for $B_s^0 \to \phi\gamma$*, *Phys. Rev. D* **91** (2015) 011101 [arXiv:1411.7771] [INSPIRE].

[3] LHCb collaboration, *First experimental study of photon polarization in radiative B_s^0 decays*, *Phys. Rev. Lett.* **118** (2017) 021801 [*Addendum ibid.* **118** (2017) 109901] [arXiv:1609.02032] [INSPIRE].

[4] LHCb collaboration, *Measurement of CP-violating and mixing-induced observables in $B_s^0 \to \phi\gamma$ decays*, *Phys. Rev. Lett.* **123** (2019) 081802 [arXiv:1905.06284] [INSPIRE].

[5] LHCb collaboration, *Strong constraints on the $b \to s\gamma$ photon polarisation from $B^0 \to K^{*0}e^+e^-$ decays*, *JHEP* **12** (2020) 081 [arXiv:2010.06011] [INSPIRE].

[6] T. Mannel and S. Recksiegel, *Flavor changing neutral current decays of heavy baryons: the case $\Lambda_b \to \Lambda\gamma$*, *J. Phys. G* **24** (1998) 979 [hep-ph/9701399] [INSPIRE].

[7] LHCb collaboration, *First observation of the radiative decay $\Lambda_b^0 \to \Lambda\gamma$*, *Phys. Rev. Lett.* **123** (2019) 031801 [arXiv:1904.06697] [INSPIRE].

[8] LHCb collaboration, *Measurement of b hadron fractions in 13 TeV pp collisions*, *Phys. Rev. D* **100** (2019) 031102 [arXiv:1902.06794] [INSPIRE].

[9] LHCb collaboration, *Measurement of the mass and production rate of Ξ_b^- baryons*, *Phys. Rev. D* **99** (2019) 052006 [arXiv:1901.07075] [INSPIRE].

[10] Y.-L. Liu, L.-F. Gan and M.-Q. Huang, *The exclusive rare decay $b \to s\gamma$ of heavy b-baryons*, *Phys. Rev. D* **83** (2011) 054007 [arXiv:1103.0081] [INSPIRE].

[11] BELLE collaboration, *Radiative B meson decays into $K\pi\gamma$ and $K\pi\pi\gamma$ final states*, *Phys. Rev. Lett.* **89** (2002) 231801 [hep-ex/0205025] [INSPIRE].

[12] LHCb collaboration, *Measurement of the ratio of branching fractions $BR(B_0 \to K^{\star 0}\gamma)/BR(B_{s0} \to \phi\gamma)$ and the direct CP asymmetry in $B_0 \to K^{\star 0}\gamma$*, *Nucl. Phys. B* **867** (2013) 1 [arXiv:1209.0313] [INSPIRE].

JHEP01(2022)069

[13] R.-M. Wang, X.-D. Cheng, Y.-Y. Fan, J.-L. Zhang and Y.-G. Xu, *Studying radiative baryon decays with the* SU(3) *flavor symmetry*, *J. Phys. G* **48** (2021) 085001 [arXiv:2008.06624] [INSPIRE].

[14] K. Azizi, Y. Sarac and H. Sundu, *Light cone QCD sum rules study of the semileptonic heavy Ξ_Q and Ξ'_Q transitions to Ξ and Σ baryons*, *Eur. Phys. J. A* **48** (2012) 2 [arXiv:1107.5925] [INSPIRE].

[15] L.M. García Martín et al., *Radiative b-baryon decays to measure the photon and b-baryon polarization*, *Eur. Phys. J. C* **79** (2019) 634 [arXiv:1902.04870] [INSPIRE].

[16] LHCb collaboration, *The LHCb detector at the LHC*, 2008 *JINST* **3** S08005 [INSPIRE].

[17] LHCb collaboration, *LHCb detector performance*, *Int. J. Mod. Phys. A* **30** (2015) 1530022 [arXiv:1412.6352] [INSPIRE].

[18] M. Kucharczyk, P. Morawski and M. Witek, *Primary vertex reconstruction at LHCb*, Tech. Rep. LHCb-PUB-2014-044, CERN, Geneva, Switzerland (2014) [CERN-LHCb-PUB-2014-044].

[19] LHCb collaboration, *Design and performance of the LHCb trigger and full real-time reconstruction in run* 2 *of the LHC*, 2019 *JINST* **14** P04013 [arXiv:1812.10790] [INSPIRE].

[20] T. Sjöstrand, S. Mrenna and P.Z. Skands, *A brief introduction to PYTHIA* 8.1, *Comput. Phys. Commun.* **178** (2008) 852 [arXiv:0710.3820] [INSPIRE].

[21] T. Sjöstrand, S. Mrenna and P.Z. Skands, *PYTHIA* 6.4 *physics and manual*, *JHEP* **05** (2006) 026 [hep-ph/0603175] [INSPIRE].

[22] LHCb collaboration, *Handling of the generation of primary events in Gauss, the LHCb simulation framework*, *J. Phys. Conf. Ser.* **331** (2011) 032047 [INSPIRE].

[23] D.J. Lange, *The EvtGen particle decay simulation package*, *Nucl. Instrum. Meth. A* **462** (2001) 152 [INSPIRE].

[24] N. Davidson, T. Przedzinski and Z. Was, *PHOTOS interface in C++: technical and physics documentation*, *Comput. Phys. Commun.* **199** (2016) 86 [arXiv:1011.0937] [INSPIRE].

[25] J. Allison et al., *GEANT4 developments and applications*, *IEEE Trans. Nucl. Sci.* **53** (2006) 270 [INSPIRE].

[26] GEANT4 collaboration, *GEANT4 — a simulation toolkit*, *Nucl. Instrum. Meth. A* **506** (2003) 250 [INSPIRE].

[27] LHCb collaboration, *The LHCb simulation application, Gauss: design, evolution and experience*, *J. Phys. Conf. Ser.* **331** (2011) 032023 [INSPIRE].

[28] D. Müller, M. Clemencic, G. Corti and M. Gersabeck, *ReDecay: a novel approach to speed up the simulation at LHCb*, *Eur. Phys. J. C* **78** (2018) 1009 [arXiv:1810.10362] [INSPIRE].

[29] R. Aaij et al., *Selection and processing of calibration samples to measure the particle identification performance of the LHCb experiment in run* 2, *EPJ Tech. Instrum.* **6** (2019) 1 [arXiv:1803.00824] [INSPIRE].

[30] Particle Data Group collaboration, *Review of particle physics*, *PTEP* **2020** (2020) 083C01 [INSPIRE].

[31] M. Calvo Gomez et al., *A tool for γ/π^0 separation at high energies*, Tech. Rep. LHCb-PUB-2015-016, CERN, Geneva, Switzerland (2015).

JHEP01(2022)069

[32] L. Breiman, J.H. Friedman, R.A. Olshen and C.J. Stone, *Classification and regression trees*, Wadsworth international group, Belmont, CA, U.S.A. (1984).

[33] T. Chen and C. Guestrin, *XGBoost: a scalable tree boosting system*, arXiv:1603.02754 [INSPIRE].

[34] M.W. Browne, *Cross-validation methods*, *J. Math. Psychol.* **44** (2000) 108.

[35] LHCb collaboration, *Observation of the suppressed decay* $\Lambda_b^0 \to p\pi^-\mu^+\mu^-$, *JHEP* **04** (2017) 029 [arXiv:1701.08705] [INSPIRE].

[36] G. Punzi, *Sensitivity of searches for new signals and its optimization*, *eConf* **C 030908** (2003) MODT002 [physics/0308063] [INSPIRE].

[37] T. Skwarnicki, *A study of the radiative cascade transitions between the Upsilon-prime and Upsilon resonances*, Ph.D. thesis, Institute of Nuclear Physics, Krakow, Poland (1986).

[38] M.B. Voloshin, *Remarks on measurement of the decay* $\Xi_b^- \to \Lambda_b\pi^-$, arXiv:1510.05568 [INSPIRE].

[39] D0 collaboration, *Measurement of the production fraction times branching fraction* $f(b \to \Lambda_b) \cdot \mathcal{B}(\Lambda_b \to J/\psi\Lambda)$, *Phys. Rev. D* **84** (2011) 031102 [arXiv:1105.0690] [INSPIRE].

[40] HFLAV collaboration, *Averages of b-hadron, c-hadron, and* τ*-lepton properties as of* 2018, *Eur. Phys. J. C* **81** (2021) 226 [arXiv:1909.12524] [INSPIRE].

[41] G.J. Feldman and R.D. Cousins, *A unified approach to the classical statistical analysis of small signals*, *Phys. Rev. D* **57** (1998) 3873 [physics/9711021] [INSPIRE].

JHEP01(2022)069

The LHCb collaboration

R. Aaij[32], A.S.W. Abdelmotteleb[56], C. Abellán Beteta[50], T. Ackernley[60], B. Adeva[46], M. Adinolfi[54], H. Afsharnia[9], C.A. Aidala[86], S. Aiola[25], Z. Ajaltouni[9], S. Akar[65], J. Albrecht[15], F. Alessio[48], M. Alexander[59], A. Alfonso Albero[45], Z. Aliouche[62], G. Alkhazov[38], P. Alvarez Cartelle[55], S. Amato[2], J.L. Amey[54], Y. Amhis[11], L. An[48], L. Anderlini[22], A. Andreianov[38], M. Andreotti[21], F. Archilli[17], A. Artamonov[44], M. Artuso[68], K. Arzymatov[42], E. Aslanides[10], M. Atzeni[50], B. Audurier[12], S. Bachmann[17], M. Bachmayer[49], J.J. Back[56], P. Baladron Rodriguez[46], V. Balagura[12], W. Baldini[21], J. Baptista Leite[1], R.J. Barlow[62], S. Barsuk[11], W. Barter[61], M. Bartolini[24,h], F. Baryshnikov[83], J.M. Basels[14], S. Bashir[34], G. Bassi[29], B. Batsukh[68], A. Battig[15], A. Bay[49], A. Beck[56], M. Becker[15], F. Bedeschi[29], I. Bediaga[1], A. Beiter[68], V. Belavin[42], S. Belin[27], V. Bellee[50], K. Belous[44], I. Belov[40], I. Belyaev[41], G. Bencivenni[23], E. Ben-Haim[13], A. Berezhnoy[40], R. Bernet[50], D. Berninghoff[17], H.C. Bernstein[68], C. Bertella[48], A. Bertolin[28], C. Betancourt[50], F. Betti[48], Ia. Bezshyiko[50], S. Bhasin[54], J. Bhom[35], L. Bian[73], M.S. Bieker[15], S. Bifani[53], P. Billoir[13], M. Birch[61], F.C.R. Bishop[55], A. Bitadze[62], A. Bizzeti[22,k], M. Bjørn[63], M.P. Blago[48], T. Blake[56], F. Blanc[49], S. Blusk[68], D. Bobulska[59], J.A. Boelhauve[15], O. Boente Garcia[46], T. Boettcher[65], A. Boldyrev[82], A. Bondar[43], N. Bondar[38,48], S. Borghi[62], M. Borisyak[42], M. Borsato[17], J.T. Borsuk[35], S.A. Bouchiba[49], T.J.V. Bowcock[60], A. Boyer[48], C. Bozzi[21], M.J. Bradley[61], S. Braun[66], A. Brea Rodriguez[46], M. Brodski[48], J. Brodzicka[35], A. Brossa Gonzalo[56], D. Brundu[27], A. Buonaura[50], L. Buonincontri[28], A.T. Burke[62], C. Burr[48], A. Bursche[72], A. Butkevich[39], J.S. Butter[32], J. Buytaert[48], W. Byczynski[48], S. Cadeddu[27], H. Cai[73], R. Calabrese[21,f], L. Calefice[15,13], L. Calero Diaz[23], S. Cali[23], R. Calladine[53], M. Calvi[26,j], M. Calvo Gomez[85], P. Camargo Magalhaes[54], P. Campana[23], A.F. Campoverde Quezada[6], S. Capelli[26,j], L. Capriotti[20,d], A. Carbone[20,d], G. Carboni[31], R. Cardinale[24,h], A. Cardini[27], I. Carli[4], P. Carniti[26,j], L. Carus[14], K. Carvalho Akiba[32], A. Casais Vidal[46], G. Casse[60], M. Cattaneo[48], G. Cavallero[48], S. Celani[49], J. Cerasoli[10], D. Cervenkov[63], A.J. Chadwick[60], M.G. Chapman[54], M. Charles[13], Ph. Charpentier[48], G. Chatzikonstantinidis[53], C.A. Chavez Barajas[60], M. Chefdeville[8], C. Chen[3], S. Chen[4], A. Chernov[35], V. Chobanova[46], S. Cholak[49], M. Chrzaszcz[35], A. Chubykin[38], V. Chulikov[38], P. Ciambrone[23], M.F. Cicala[56], X. Cid Vidal[46], G. Ciezarek[48], P.E.L. Clarke[58], M. Clemencic[48], H.V. Cliff[55], J. Closier[48], J.L. Cobbledick[62], V. Coco[48], J.A.B. Coelho[11], J. Cogan[10], E. Cogneras[9], L. Cojocariu[37], P. Collins[48], T. Colombo[48], L. Congedo[19,c], A. Contu[27], N. Cooke[53], G. Coombs[59], I. Corredoira [46], G. Corti[48], C.M. Costa Sobral[56], B. Couturier[48], D.C. Craik[64], J. Crkovská[67], M. Cruz Torres[1], R. Currie[58], C.L. Da Silva[67], S. Dadabaev[83], L. Dai[71], E. Dall'Occo[15], J. Dalseno[46], C. D'Ambrosio[48], A. Danilina[41], P. d'Argent[48], J.E. Davies[62], A. Davis[62], O. De Aguiar Francisco[62], K. De Bruyn[79], S. De Capua[62], M. De Cian[49], J.M. De Miranda[1], L. De Paula[2], M. De Serio[19,c], D. De Simone[50], P. De Simone[23], J.A. de Vries[80], C.T. Dean[67], D. Decamp[8], L. Del Buono[13], B. Delaney[55], H.-P. Dembinski[15], A. Dendek[34], V. Denysenko[50], D. Derkach[82], O. Deschamps[9], F. Desse[11], F. Dettori[27,e], B. Dey[77], A. Di Cicco[23], P. Di Nezza[23], S. Didenko[83], L. Dieste Maronas[46], H. Dijkstra[48], V. Dobishuk[52], C. Dong[3], A.M. Donohoe[18], F. Dordei[27], A.C. dos Reis[1], L. Douglas[59], A. Dovbnya[51], A.G. Downes[8], M.W. Dudek[35], L. Dufour[48], V. Duk[78], P. Durante[48], J.M. Durham[67], D. Dutta[62], A. Dziurda[35], A. Dzyuba[38], S. Easo[57], U. Egede[69], V. Egorychev[41], S. Eidelman[43,v], S. Eisenhardt[58], S. Ek-In[49], L. Eklund[59,w], S. Ely[68], A. Ene[37], E. Epple[67], S. Escher[14], J. Eschle[50], S. Esen[13], T. Evans[48], A. Falabella[20], J. Fan[3], Y. Fan[6], B. Fang[73], S. Farry[60], D. Fazzini[26,j], M. Féo[48], A. Fernandez Prieto[46], A.D. Fernez[66], F. Ferrari[20,d], L. Ferreira Lopes[49], F. Ferreira Rodrigues[2], S. Ferreres Sole[32], M. Ferrillo[50], M. Ferro-Luzzi[48], S. Filippov[39], R.A. Fini[19], M. Fiorini[21,f],

JHEP01(2022)069

M. Firlej[34], K.M. Fischer[63], D.S. Fitzgerald[86], C. Fitzpatrick[62], T. Fiutowski[34], A. Fkiaras[48], F. Fleuret[12], M. Fontana[13], F. Fontanelli[24,h], R. Forty[48], D. Foulds-Holt[55], V. Franco Lima[60], M. Franco Sevilla[66], M. Frank[48], E. Franzoso[21], G. Frau[17], C. Frei[48], D.A. Friday[59], J. Fu[25], Q. Fuehring[15], W. Funk[48], E. Gabriel[32], T. Gaintseva[42], A. Gallas Torreira[46], D. Galli[20,d], S. Gambetta[58,48], Y. Gan[3], M. Gandelman[2], P. Gandini[25], Y. Gao[5], M. Garau[27], L.M. Garcia Martin[56], P. Garcia Moreno[45], J. García Pardiñas[26,j], B. Garcia Plana[46], F.A. Garcia Rosales[12], L. Garrido[45], C. Gaspar[48], R.E. Geertsema[32], D. Gerick[17], L.L. Gerken[15], E. Gersabeck[62], M. Gersabeck[62], T. Gershon[56], D. Gerstel[10], Ph. Ghez[8], V. Gibson[55], H.K. Giemza[36], A.L. Gilman[63], M. Giovannetti[23,p], A. Gioventù[46], P. Gironella Gironell[45], L. Giubega[37], C. Giugliano[21,f,48], K. Gizdov[58], E.L. Gkougkousis[48], V.V. Gligorov[13], C. Göbel[70], E. Golobardes[85], D. Golubkov[41], A. Golutvin[61,83], A. Gomes[1,a], S. Gomez Fernandez[45], F. Goncalves Abrantes[63], M. Goncerz[35], G. Gong[3], P. Gorbounov[41], I.V. Gorelov[40], C. Gotti[26], E. Govorkova[48], J.P. Grabowski[17], T. Grammatico[13], L.A. Granado Cardoso[48], E. Graugés[45], E. Graverini[49], G. Graziani[22], A. Grecu[37], L.M. Greeven[32], N.A. Grieser[4], P. Griffith[21,f], L. Grillo[62], S. Gromov[83], B.R. Gruberg Cazon[63], C. Gu[3], M. Guarise[21], P. A. Günther[17], E. Gushchin[39], A. Guth[14], Y. Guz[44], T. Gys[48], T. Hadavizadeh[69], G. Haefeli[49], C. Haen[48], J. Haimberger[48], T. Halewood-leagas[60], P.M. Hamilton[66], J.P. Hammerich[60], Q. Han[7], X. Han[17], T.H. Hancock[63], S. Hansmann-Menzemer[17], N. Harnew[63], T. Harrison[60], C. Hasse[48], M. Hatch[48], J. He[6,b], M. Hecker[61], K. Heijhoff[32], K. Heinicke[15], A.M. Hennequin[48], K. Hennessy[60], L. Henry[48], J. Heuel[14], A. Hicheur[2], D. Hill[49], M. Hilton[62], S.E. Hollitt[15], J. Hu[17], J. Hu[72], W. Hu[7], X. Hu[3], W. Huang[6], X. Huang[73], W. Hulsbergen[32], R.J. Hunter[56], M. Hushchyn[82], D. Hutchcroft[60], D. Hynds[32], P. Ibis[15], M. Idzik[34], D. Ilin[38], P. Ilten[65], A. Inglessi[38], A. Ishteev[83], K. Ivshin[38], R. Jacobsson[48], S. Jakobsen[48], E. Jans[32], B.K. Jashal[47], A. Jawahery[66], V. Jevtic[15], F. Jiang[3], M. John[63], D. Johnson[48], C.R. Jones[55], T.P. Jones[56], B. Jost[48], N. Jurik[48], S.H. Kalavan Kadavath[34], S. Kandybei[51], Y. Kang[3], M. Karacson[48], M. Karpov[82], F. Keizer[48], M. Kenzie[56], T. Ketel[33], B. Khanji[15], A. Kharisova[84], S. Kholodenko[44], T. Kirn[14], V.S. Kirsebom[49], O. Kitouni[64], S. Klaver[32], K. Klimaszewski[36], M.R. Kmiec[36], S. Koliiev[52], A. Kondybayeva[83], A. Konoplyannikov[41], P. Kopciewicz[34], R. Kopecna[17], P. Koppenburg[32], M. Korolev[40], I. Kostiuk[32,52], O. Kot[52], S. Kotriakhova[21,38], P. Kravchenko[38], L. Kravchuk[39], R.D. Krawczyk[48], M. Kreps[56], F. Kress[61], S. Kretzschmar[14], P. Krokovny[43,v], W. Krupa[34], W. Krzemien[36], W. Kucewicz[35,t], M. Kucharczyk[35], V. Kudryavtsev[43,v], H.S. Kuindersma[32,33], G.J. Kunde[67], T. Kvaratskheliya[41], D. Lacarrere[48], G. Lafferty[62], A. Lai[27], A. Lampis[27], D. Lancierini[50], J.J. Lane[62], R. Lane[54], G. Lanfranchi[23], C. Langenbruch[14], J. Langer[15], O. Lantwin[83], T. Latham[56], F. Lazzari[29,q], R. Le Gac[10], S.H. Lee[86], R. Lefèvre[9], A. Leflat[40], S. Legotin[83], O. Leroy[10], T. Lesiak[35], B. Leverington[17], H. Li[72], P. Li[17], S. Li[7], Y. Li[4], Y. Li[4], Z. Li[68], X. Liang[68], T. Lin[61], R. Lindner[48], V. Lisovskyi[15], R. Litvinov[27], G. Liu[72], H. Liu[6], S. Liu[4], A. Lobo Salvia[45], A. Loi[27], J. Lomba Castro[46], I. Longstaff[59], J.H. Lopes[2], S. Lopez Solino[46], G.H. Lovell[55], Y. Lu[4], D. Lucchesi[28,l], S. Luchuk[39], M. Lucio Martinez[32], V. Lukashenko[32,52], Y. Luo[3], A. Lupato[62], E. Luppi[21,f], O. Lupton[56], A. Lusiani[29,m], X. Lyu[6], L. Ma[4], R. Ma[6], S. Maccolini[20,d], F. Machefert[11], F. Maciuc[37], V. Macko[49], P. Mackowiak[15], S. Maddrell-Mander[54], O. Madejczyk[34], L.R. Madhan Mohan[54], O. Maev[38], A. Maevskiy[82], D. Maisuzenko[38], M.W. Majewski[34], J.J. Malczewski[35], S. Malde[63], B. Malecki[48], A. Malinin[81], T. Maltsev[43,v], H. Malygina[17], G. Manca[27,e], G. Mancinelli[10], D. Manuzzi[20,d], D. Marangotto[25,i], J. Maratas[9,s], J.F. Marchand[8], U. Marconi[20], S. Mariani[22,g], C. Marin Benito[48], M. Marinangeli[49], J. Marks[17], A.M. Marshall[54], P.J. Marshall[60], G. Martellotti[30], L. Martinazzoli[48,j], M. Martinelli[26,j], D. Martinez Santos[46], F. Martinez Vidal[47], A. Massafferri[1], M. Materok[14], R. Matev[48], A. Mathad[50], Z. Mathe[48], V. Matiunin[41], C. Matteuzzi[26], K.R. Mattioli[86], A. Mauri[32], E. Maurice[12], J. Mauricio[45], M. Mazurek[48], M. McCann[61],

JHEP01(2022)069

L. Mcconnell[18], T.H. Mcgrath[62], N.T. Mchugh[59], A. McNab[62], R. McNulty[18], J.V. Mead[60], B. Meadows[65], G. Meier[15], N. Meinert[76], D. Melnychuk[36], S. Meloni[26,j], M. Merk[32,80], A. Merli[25], L. Meyer Garcia[2], M. Mikhasenko[48], D.A. Milanes[74], E. Millard[56], M. Milovanovic[48], M.-N. Minard[8], A. Minotti[21], L. Minzoni[21,f], S.E. Mitchell[58], B. Mitreska[62], D.S. Mitzel[48], A. Mödden [15], R.A. Mohammed[63], R.D. Moise[61], T. Mombächer[46], I.A. Monroy[74], S. Monteil[9], M. Morandin[28], G. Morello[23], M.J. Morello[29,m], J. Moron[34], A.B. Morris[75], A.G. Morris[56], R. Mountain[68], H. Mu[3], F. Muheim[58,48], M. Mulder[48], D. Müller[48], K. Müller[50], C.H. Murphy[63], D. Murray[62], P. Muzzetto[27,48], P. Naik[54], T. Nakada[49], R. Nandakumar[57], T. Nanut[49], I. Nasteva[2], M. Needham[58], I. Neri[21], N. Neri[25,i], S. Neubert[75], N. Neufeld[48], R. Newcombe[61], T.D. Nguyen[49], C. Nguyen-Mau[49,x], E.M. Niel[11], S. Nieswand[14], N. Nikitin[40], N.S. Nolte[64], C. Normand[8], C. Nunez[86], A. Oblakowska-Mucha[34], V. Obraztsov[44], T. Oeser[14], D.P. O'Hanlon[54], S. Okamura[21], R. Oldeman[27,e], M.E. Olivares[68], C.J.G. Onderwater[79], R.H. O'neil[58], A. Ossowska[35], J.M. Otalora Goicochea[2], T. Ovsiannikova[41], P. Owen[50], A. Oyanguren[47], K.O. Padeken[75], B. Pagare[56], P.R. Pais[48], T. Pajero[63], A. Palano[19], M. Palutan[23], Y. Pan[62], G. Panshin[84], A. Papanestis[57], M. Pappagallo[19,c], L.L. Pappalardo[21,f], C. Pappenheimer[65], W. Parker[66], C. Parkes[62], B. Passalacqua[21], G. Passaleva[22], A. Pastore[19], M. Patel[61], C. Patrignani[20,d], C.J. Pawley[80], A. Pearce[48], A. Pellegrino[32], M. Pepe Altarelli[48], S. Perazzini[20], D. Pereima[41], A. Pereiro Castro[46], P. Perret[9], M. Petric[59,48], K. Petridis[54], A. Petrolini[24,h], A. Petrov[81], S. Petrucci[58], M. Petruzzo[25], T.T.H. Pham[68], A. Philippov[42], L. Pica[29,m], M. Piccini[78], B. Pietrzyk[8], G. Pietrzyk[49], M. Pili[63], D. Pinci[30], F. Pisani[48], M. Pizzichemi[26,48,j], Resmi P.K[10], V. Placinta[37], J. Plews[53], M. Plo Casasus[46], F. Polci[13], M. Poli Lener[23], M. Poliakova[68], A. Poluektov[10], N. Polukhina[83,u], I. Polyakov[68], E. Polycarpo[2], S. Ponce[48], D. Popov[6,48], S. Popov[42], S. Poslavskii[44], K. Prasanth[35], L. Promberger[48], C. Prouve[46], V. Pugatch[52], V. Puill[11], H. Pullen[63], G. Punzi[29,n], H. Qi[3], W. Qian[6], J. Qin[6], N. Qin[3], R. Quagliani[13], B. Quintana[8], N.V. Raab[18], R.I. Rabadan Trejo[10], B. Rachwal[34], J.H. Rademacker[54], M. Rama[29], M. Ramos Pernas[56], M.S. Rangel[2], F. Ratnikov[42,82], G. Raven[33], M. Reboud[8], F. Redi[49], F. Reiss[62], C. Remon Alepuz[47], Z. Ren[3], V. Renaudin[63], R. Ribatti[29], S. Ricciardi[57], K. Rinnert[60], P. Robbe[11], G. Robertson[58], A.B. Rodrigues[49], E. Rodrigues[60], J.A. Rodriguez Lopez[74], E.R.R. Rodriguez Rodriguez[46], A. Rollings[63], P. Roloff[48], V. Romanovskiy[44], M. Romero Lamas[46], A. Romero Vidal[46], J.D. Roth[86], M. Rotondo[23], M.S. Rudolph[68], T. Ruf[48], R.A. Ruiz Fernandez[46], J. Ruiz Vidal[47], A. Ryzhikov[82], J. Ryzka[34], J.J. Saborido Silva[46], N. Sagidova[38], N. Sahoo[56], B. Saitta[27,e], M. Salomoni[48], C. Sanchez Gras[32], R. Santacesaria[30], C. Santamarina Rios[46], M. Santimaria[23], E. Santovetti[31,p], D. Saranin[83], G. Sarpis[14], M. Sarpis[75], A. Sarti[30], C. Satriano[30,o], A. Satta[31], M. Saur[15], D. Savrina[41,40], H. Sazak[9], L.G. Scantlebury Smead[63], A. Scarabotto[13], S. Schael[14], S. Scherl[60], M. Schiller[59], H. Schindler[48], M. Schmelling[16], B. Schmidt[48], O. Schneider[49], A. Schopper[48], M. Schubiger[32], S. Schulte[49], M.H. Schune[11], R. Schwemmer[48], B. Sciascia[23], S. Sellam[46], A. Semennikov[41], M. Senghi Soares[33], A. Sergi[24,h], N. Serra[50], L. Sestini[28], A. Seuthe[15], P. Seyfert[48], Y. Shang[5], D.M. Shangase[86], M. Shapkin[44], I. Shchemerov[83], L. Shchutska[49], T. Shears[60], L. Shekhtman[43,v], Z. Shen[5], V. Shevchenko[81], E.B. Shields[26,j], Y. Shimizu[11], E. Shmanin[83], J.D. Shupperd[68], B.G. Siddi[21], R. Silva Coutinho[50], G. Simi[28], S. Simone[19,c], N. Skidmore[62], T. Skwarnicki[68], M.W. Slater[53], I. Slazyk[21,f], J.C. Smallwood[63], J.G. Smeaton[55], A. Smetkina[41], E. Smith[50], M. Smith[61], A. Snoch[32], M. Soares[20], L. Soares Lavra[9], M.D. Sokoloff[65], F.J.P. Soler[59], A. Solovev[38], I. Solovyev[38], F.L. Souza De Almeida[2], B. Souza De Paula[2], B. Spaan[15], E. Spadaro Norella[25], P. Spradlin[59], F. Stagni[48], M. Stahl[65], S. Stahl[48], S. Stanislaus[63], O. Steinkamp[50,83], O. Stenyakin[44], H. Stevens[15], S. Stone[68], M.E. Stramaglia[49], M. Straticiuc[37], D. Strekalina[83], F. Suljik[63], J. Sun[27], L. Sun[73], Y. Sun[66], P. Svihra[62], P.N. Swallow[53], K. Swientek[34], A. Szabelski[36], T. Szumlak[34], M. Szymanski[48], S. Taneja[62], A.R. Tanner[54],

JHEP01(2022)069

M.D. Tat[63], A. Terentev[83], F. Teubert[48], E. Thomas[48], D.J.D. Thompson[53], K.A. Thomson[60], V. Tisserand[9], S. T'Jampens[8], M. Tobin[4], L. Tomassetti[21,f], X. Tong[5], D. Torres Machado[1], D.Y. Tou[13], M.T. Tran[49], E. Trifonova[83], C. Trippl[49], G. Tuci[29,n], A. Tully[49], N. Tuning[32,48], A. Ukleja[36], D.J. Unverzagt[17], E. Ursov[83], A. Usachov[32], A. Ustyuzhanin[42,82], U. Uwer[17], A. Vagner[84], V. Vagnoni[20], A. Valassi[48], G. Valenti[20], N. Valls Canudas[85], M. van Beuzekom[32], M. Van Dijk[49], E. van Herwijnen[83], C.B. Van Hulse[18], M. van Veghel[79], R. Vazquez Gomez[45], P. Vazquez Regueiro[46], C. Vázquez Sierra[48], S. Vecchi[21], J.J. Velthuis[54], M. Veltri[22,r], A. Venkateswaran[68], M. Veronesi[32], M. Vesterinen[56], D. Vieira[65], M. Vieites Diaz[49], H. Viemann[76], X. Vilasis-Cardona[85], E. Vilella Figueras[60], A. Villa[20], P. Vincent[13], F.C. Volle[11], D. Vom Bruch[10], A. Vorobyev[38], V. Vorobyev[43,v], N. Voropaev[38], K. Vos[80], R. Waldi[17], J. Walsh[29], C. Wang[17], J. Wang[5], J. Wang[4], J. Wang[3], J. Wang[73], M. Wang[3], R. Wang[54], Y. Wang[7], Z. Wang[50], Z. Wang[3], J.A. Ward[56], H.M. Wark[60], N.K. Watson[53], S.G. Weber[13], D. Websdale[61], C. Weisser[64], B.D.C. Westhenry[54], D.J. White[62], M. Whitehead[54], A.R. Wiederhold[56], D. Wiedner[15], G. Wilkinson[63], M. Wilkinson[68], I. Williams[55], M. Williams[64], M.R.J. Williams[58], F.F. Wilson[57], W. Wislicki[36], M. Witek[35], L. Witola[17], G. Wormser[11], S.A. Wotton[55], H. Wu[68], K. Wyllie[48], Z. Xiang[6], D. Xiao[7], Y. Xie[7], A. Xu[5], J. Xu[6], L. Xu[3], M. Xu[7], Q. Xu[6], Z. Xu[5], Z. Xu[6], D. Yang[3], S. Yang[6], Y. Yang[6], Z. Yang[5], Z. Yang[66], Y. Yao[68], L.E. Yeomans[60], H. Yin[7], J. Yu[71], X. Yuan[68], O. Yushchenko[44], E. Zaffaroni[49], M. Zavertyaev[16,u], M. Zdybal[35], O. Zenaiev[48], M. Zeng[3], D. Zhang[7], L. Zhang[3], S. Zhang[71], S. Zhang[5], Y. Zhang[5], Y. Zhang[63], A. Zharkova[83], A. Zhelezov[17], Y. Zheng[6], T. Zhou[5], X. Zhou[6], Y. Zhou[6], V. Zhovkovska[11], X. Zhu[3], Z. Zhu[6], V. Zhukov[14,40], J.B. Zonneveld[58], Q. Zou[4], S. Zucchelli[20,d], D. Zuliani[28] and G. Zunica[62]

[1] *Centro Brasileiro de Pesquisas Físicas (CBPF), Rio de Janeiro, Brazil*
[2] *Universidade Federal do Rio de Janeiro (UFRJ), Rio de Janeiro, Brazil*
[3] *Center for High Energy Physics, Tsinghua University, Beijing, China*
[4] *Institute Of High Energy Physics (IHEP), Beijing, China*
[5] *School of Physics State Key Laboratory of Nuclear Physics and Technology, Peking University, Beijing, China*
[6] *University of Chinese Academy of Sciences, Beijing, China*
[7] *Institute of Particle Physics, Central China Normal University, Wuhan, Hubei, China*
[8] *Univ. Savoie Mont Blanc, CNRS, IN2P3-LAPP, Annecy, France*
[9] *Université Clermont Auvergne, CNRS/IN2P3, LPC, Clermont-Ferrand, France*
[10] *Aix Marseille Univ, CNRS/IN2P3, CPPM, Marseille, France*
[11] *Université Paris-Saclay, CNRS/IN2P3, IJCLab, Orsay, France*
[12] *Laboratoire Leprince-Ringuet, CNRS/IN2P3, Ecole Polytechnique, Institut Polytechnique de Paris, Palaiseau, France*
[13] *LPNHE, Sorbonne Université, Paris Diderot Sorbonne Paris Cité, CNRS/IN2P3, Paris, France*
[14] *I. Physikalisches Institut, RWTH Aachen University, Aachen, Germany*
[15] *Fakultät Physik, Technische Universität Dortmund, Dortmund, Germany*
[16] *Max-Planck-Institut für Kernphysik (MPIK), Heidelberg, Germany*
[17] *Physikalisches Institut, Ruprecht-Karls-Universität Heidelberg, Heidelberg, Germany*
[18] *School of Physics, University College Dublin, Dublin, Ireland*
[19] *INFN Sezione di Bari, Bari, Italy*
[20] *INFN Sezione di Bologna, Bologna, Italy*
[21] *INFN Sezione di Ferrara, Ferrara, Italy*
[22] *INFN Sezione di Firenze, Firenze, Italy*
[23] *INFN Laboratori Nazionali di Frascati, Frascati, Italy*
[24] *INFN Sezione di Genova, Genova, Italy*
[25] *INFN Sezione di Milano, Milano, Italy*

JHEP01(2022)069

[26] INFN Sezione di Milano-Bicocca, Milano, Italy
[27] INFN Sezione di Cagliari, Monserrato, Italy
[28] Universita degli Studi di Padova, Universita e INFN, Padova, Padova, Italy
[29] INFN Sezione di Pisa, Pisa, Italy
[30] INFN Sezione di Roma La Sapienza, Roma, Italy
[31] INFN Sezione di Roma Tor Vergata, Roma, Italy
[32] Nikhef National Institute for Subatomic Physics, Amsterdam, Netherlands
[33] Nikhef National Institute for Subatomic Physics and VU University Amsterdam, Amsterdam, Netherlands
[34] AGH — University of Science and Technology, Faculty of Physics and Applied Computer Science, Kraków, Poland
[35] Henryk Niewodniczanski Institute of Nuclear Physics Polish Academy of Sciences, Kraków, Poland
[36] National Center for Nuclear Research (NCBJ), Warsaw, Poland
[37] Horia Hulubei National Institute of Physics and Nuclear Engineering, Bucharest-Magurele, Romania
[38] Petersburg Nuclear Physics Institute NRC Kurchatov Institute (PNPI NRC KI), Gatchina, Russia
[39] Institute for Nuclear Research of the Russian Academy of Sciences (INR RAS), Moscow, Russia
[40] Institute of Nuclear Physics, Moscow State University (SINP MSU), Moscow, Russia
[41] Institute of Theoretical and Experimental Physics NRC Kurchatov Institute (ITEP NRC KI), Moscow, Russia
[42] Yandex School of Data Analysis, Moscow, Russia
[43] Budker Institute of Nuclear Physics (SB RAS), Novosibirsk, Russia
[44] Institute for High Energy Physics NRC Kurchatov Institute (IHEP NRC KI), Protvino, Russia, Protvino, Russia
[45] ICCUB, Universitat de Barcelona, Barcelona, Spain
[46] Instituto Galego de Física de Altas Enerxías (IGFAE), Universidade de Santiago de Compostela, Santiago de Compostela, Spain
[47] Instituto de Fisica Corpuscular, Centro Mixto Universidad de Valencia — CSIC, Valencia, Spain
[48] European Organization for Nuclear Research (CERN), Geneva, Switzerland
[49] Institute of Physics, Ecole Polytechnique Fédérale de Lausanne (EPFL), Lausanne, Switzerland
[50] Physik-Institut, Universität Zürich, Zürich, Switzerland
[51] NSC Kharkiv Institute of Physics and Technology (NSC KIPT), Kharkiv, Ukraine
[52] Institute for Nuclear Research of the National Academy of Sciences (KINR), Kyiv, Ukraine
[53] University of Birmingham, Birmingham, United Kingdom
[54] H.H. Wills Physics Laboratory, University of Bristol, Bristol, United Kingdom
[55] Cavendish Laboratory, University of Cambridge, Cambridge, United Kingdom
[56] Department of Physics, University of Warwick, Coventry, United Kingdom
[57] STFC Rutherford Appleton Laboratory, Didcot, United Kingdom
[58] School of Physics and Astronomy, University of Edinburgh, Edinburgh, United Kingdom
[59] School of Physics and Astronomy, University of Glasgow, Glasgow, United Kingdom
[60] Oliver Lodge Laboratory, University of Liverpool, Liverpool, United Kingdom
[61] Imperial College London, London, United Kingdom
[62] Department of Physics and Astronomy, University of Manchester, Manchester, United Kingdom
[63] Department of Physics, University of Oxford, Oxford, United Kingdom
[64] Massachusetts Institute of Technology, Cambridge, MA, United States
[65] University of Cincinnati, Cincinnati, OH, United States
[66] University of Maryland, College Park, MD, United States
[67] Los Alamos National Laboratory (LANL), Los Alamos, United States
[68] Syracuse University, Syracuse, NY, United States
[69] School of Physics and Astronomy, Monash University, Melbourne, Australia, associated to [56]
[70] Pontifícia Universidade Católica do Rio de Janeiro (PUC-Rio), Rio de Janeiro, Brazil, associated to [2]

JHEP01(2022)069

[71] *Physics and Micro Electronic College, Hunan University, Changsha City, China, associated to* [7]
[72] *Guangdong Provincial Key Laboratory of Nuclear Science, Guangdong-Hong Kong Joint Laboratory of Quantum Matter, Institute of Quantum Matter, South China Normal University, Guangzhou, China, associated to* [3]
[73] *School of Physics and Technology, Wuhan University, Wuhan, China, associated to* [3]
[74] *Departamento de Fisica , Universidad Nacional de Colombia, Bogota, Colombia, associated to* [13]
[75] *Universität Bonn — Helmholtz-Institut für Strahlen und Kernphysik, Bonn, Germany, associated to* [17]
[76] *Institut für Physik, Universität Rostock, Rostock, Germany, associated to* [17]
[77] *Eotvos Lorand University, Budapest, Hungary, associated to* [48]
[78] *INFN Sezione di Perugia, Perugia, Italy, associated to* [21]
[79] *Van Swinderen Institute, University of Groningen, Groningen, Netherlands, associated to* [32]
[80] *Universiteit Maastricht, Maastricht, Netherlands, associated to* [32]
[81] *National Research Centre Kurchatov Institute, Moscow, Russia, associated to* [41]
[82] *National Research University Higher School of Economics, Moscow, Russia, associated to* [42]
[83] *National University of Science and Technology "MISIS", Moscow, Russia, associated to* [41]
[84] *National Research Tomsk Polytechnic University, Tomsk, Russia, associated to* [41]
[85] *DS4DS, La Salle, Universitat Ramon Llull, Barcelona, Spain, associated to* [45]
[86] *University of Michigan, Ann Arbor, United States, associated to* [68]

[a] *Universidade Federal do Triângulo Mineiro (UFTM), Uberaba-MG, Brazil*
[b] *Hangzhou Institute for Advanced Study, UCAS, Hangzhou, China*
[c] *Università di Bari, Bari, Italy*
[d] *Università di Bologna, Bologna, Italy*
[e] *Università di Cagliari, Cagliari, Italy*
[f] *Università di Ferrara, Ferrara, Italy*
[g] *Università di Firenze, Firenze, Italy*
[h] *Università di Genova, Genova, Italy*
[i] *Università degli Studi di Milano, Milano, Italy*
[j] *Università di Milano Bicocca, Milano, Italy*
[k] *Università di Modena e Reggio Emilia, Modena, Italy*
[l] *Università di Padova, Padova, Italy*
[m] *Scuola Normale Superiore, Pisa, Italy*
[n] *Università di Pisa, Pisa, Italy*
[o] *Università della Basilicata, Potenza, Italy*
[p] *Università di Roma Tor Vergata, Roma, Italy*
[q] *Università di Siena, Siena, Italy*
[r] *Università di Urbino, Urbino, Italy*
[s] *MSU — Iligan Institute of Technology (MSU-IIT), Iligan, Philippines*
[t] *AGH — University of Science and Technology, Faculty of Computer Science, Electronics and Telecommunications, Kraków, Poland*
[u] *P.N. Lebedev Physical Institute, Russian Academy of Science (LPI RAS), Moscow, Russia*
[v] *Novosibirsk State University, Novosibirsk, Russia*
[w] *Department of Physics and Astronomy, Uppsala University, Uppsala, Sweden*
[x] *Hanoi University of Science, Hanoi, Vietnam*

JHEP01(2022)069